J Mater Sci (2008) 43:5540–5545
DOI 10.1007/s10853-008-2833-5

Microwave initiated hydrothermal synthesis of nano-sized complex fluorides, KMF_3 (K = Zn, Mn, Co, and Fe)

Purnendu Parhi · Jon Kramer · V. Manivannan

Received: 5 February 2008 / Accepted: 24 June 2008 / Published online: 9 July 2008

Abstract A microwave assisted hydrothermal method, where the advantages of both microwave and hydrothermal methods are utilized to synthesize complex fluoride KMF_3 (M = Zn, Mn, Co, Fe), materials of technological importance, is proposed. The KMF_3 metal fluorides synthesized feature nano-sized particles having well-defined cubic morphologies. The proposed synthesis, in contrast to the existing synthesis methods is very rapid, economical, and less complex in nature. The structural, thermal, optical, and chemical properties of synthesized powders are determined by powder X-ray diffraction, scanning and transmission electron microscopy, X-ray photoelectron spectroscopy, Fourier transform infrared spectroscopy, and diffuse reflectance spectra in the UV–VIS range.

Introduction

Complex fluorides KMF_3 are technologically important materials and have found applications in many electronic devices mostly due to their interesting properties associated with the perovskite-type crystal structure [1–3]. KMF_3 fluorides are prepared by a variety of methods including solid-state, mechanochemical, micro emulsion, high temperature and pressure, hydrothermal, and solvothermal techniques [4–10]. The synthesis procedure involved high temperatures, complicated and expensive set up, and complex procedures, mainly due to the corrosive nature of fluorides. Therefore, synthesis procedures that can improve the above-mentioned drawbacks are needed.

Mild hydrothermal or solvothermal processes where the reactions are performed at 140–250 °C have evolved as an effective method to synthesize KMF_3 fluorides [8, 9]. In addition, the oxygen content of the KMF_3 materials synthesized by hydrothermal and solvothermal methods is lower than that of the methods mentioned previously. However, one of the major drawbacks of the hydrothermal synthesis is the associated slow reaction kinetics for a given reaction condition [11].

Microwave energy applied during the hydrothermal synthesis [microwave-hydrothermal (M-H)] has been found to improve the kinetics of crystallization [12–14]. Microwave radiation penetrates deeply, induces the rotation of molecules and vibration of materials with dielectric properties and molecular dipole moments enabling faster chemical reaction between the precursors leading to the desired product formation [15].

High pressures (over 600 psi) as well as high temperatures (over 300 °C) could be generated in the reaction vessel during the M-H process [16]. Such reaction conditions help to homogeneously heat the reaction medium within a short period of time, resulting in products with narrow particle size distribution, high yield, high purity, and excellent reproducibility. Such a method has been employed as a synthetic tool to successfully synthesize various materials [17–20].

We have extended the microwave hydrothermal method for the successful synthesis of complex metal fluorides KMF_3 (M = Zn, Mn, Co, Fe). We have introduced further simplicity in the process by performing the reactions in simple solution state (with water as the solvent) using a

P. Parhi · J. Kramer · V. Manivannan (✉)
Department of Mechanical Engineering, Campus Delivery 1374, Colorado State University, Fort Collins, CO 80523, USA
e-mail: mani@engr.colostate.edu

domestic microwave oven and completing the reactions within a short period of time (less than 5 min). Such a method of synthesis, i.e. using M-H to synthesis KMF_3, has not been previously reported.

Experimental

KF, $ZnCl_2$, $MnCl_2 \cdot 4H_2O$, $CoCl_2 \cdot 6H_2O$, and $FeCl_2 \cdot 4H_2O$ starting materials were obtained from Alfa Aesar, USA, and were used as-received. For the synthesis of ternary metal fluorides, KF and MCl_2 (M = Zn, Mn, Co, Fe), were added in a 3:1 molar ratio into a Parr hydrothermal vessel along with 15 mL of deionized water. For example, to synthesize $KZnF_3$, 0.5 g of KF and 0.392 g of $ZnCl_2$ were used according to the reaction

$$3KF + ZnCl_2 \rightarrow KZnF_3 + 2KCl. \quad (1)$$

The Parr vessel was subjected to microwave treatment for 4 min. A domestic microwave operating at 2.45 GHz with a maximum power of 1100 W was used. After the completion of the reaction, the Parr hydrothermal vessel was allowed to cool to room temperature. The products obtained were washed with distilled water and ethanol many times and then dried on a hot plate at 90 °C overnight.

Structural properties of the materials were determined by performing multiple characterizations. X-ray diffraction (XRD) patterns were collected with a Scintag X2 diffractometer using CuK_α radiation. A scan rate of 1°/min with a step size of 0.02° was employed to obtain the XRD diffraction pattern. SEM characterization was performed on the JSM-6500F, a field emission system with the in-lens thermal field emission electron gun. X-ray photoelectron spectroscopy (XPS) experiments were performed on a Physical Electronics 5800 spectrometer. This system has a monochromatic Al K_α X-ray source ($h_\alpha = 1486.6$ eV), hemispherical analyzer, and multichannel detector. A low energy (30 eV) electron gun was used for charge neutralization on the non-conducting samples. The binding energy scales for the samples were referenced to the C1s peak at 284.8 eV. Diffuse reflectance spectra were recorded in the wavelength range of 250–2500 nm using a Varian Associates 500 double beam spectrophotometer equipped with a Praying Mantis. Compressed polytetrafluoroethylene was used for standard calibration (100% reflectance). Fourier transform infrared spectroscopy (FTIR) measurements in the 400–4000 cm^{-1} were carried out with Nicolet Magna FTIR equipped with deuterated triglycine sulfate detector. Samples for FTIR were made by pressing a mixture of KBr and powdered sample. Transmission electron microscopy (TEM) was carried out on a 2000 TEM (JEOL, Japan), operating at an accelerating voltage of 100–200 kV.

Results and discussion

Figure 1 shows the XRD pattern of the synthesized complex fluorides. Figure 1a, b, c, and d shows XRD patterns of $KZnF_3$, $KMnF_3$, $KCoF_3$, and $KFeF_3$, respectively, synthesized by the microwave hydrothermal method. Comparison of the XRD patterns with JCPDF standard showed the single-phase nature of the fluoride materials synthesized [21]. The $KFeF_3$ product contains a small quantity of an impurity phase. In general, KMF_3 (M = Zn, Mn, Co, Fe)-type fluorides belong to the perovskite ABO_3 family of materials. Crystal structure details of the synthesized fluorides are summarized in Table 1.

Figure 2 shows the SEM images of the synthesized fluorides. Figure 2a, b, c, and d shows SEM images of $KZnF_3$, $KMnF_3$, $KCoF_3$, and $KFeF_3$, respectively. Well-defined morphology is noticed for almost all the fluorides with particles in the nm size range. Specifically, $KZnF_3$, $KMnF_3$, and $KFeF_3$ have cubic-shaped particles. Small pits can be seen in the synthesized $KCoF_3$. In general, the synthesized fluorides have potassium to metal ratios of ~ 1, as determined by energy-dispersive X-ray analysis. Figure 3 shows TEM images of the synthesized fluorides. TEM images for $KZnF_3$ (Fig. 3a), $KMnF_3$ (Fig. 3b, c), $KCoF_3$ (Fig. 3d), and $KFeF_3$ (Fig. 3e), showed cubic morphologies which is in consistent with SEM observations.

Figure 4 shows the FTIR spectra of the synthesized fluorides. The results showed there was no surface adsorbed water for any of the fluorides except for $KCoF_3$. For $KCoF_3$ small peaks at 3400 cm^{-1} and 3600 cm^{-1} are noticed which indicate the presence of a small amount of surface water possibly due to insufficient drying.

XPS analysis was performed to examine the composition of the synthesized fluorides (Fig. 5). In the full spectrum analysis of $KCoF_3$ (not shown), a very weak O1s peak at 531.3 eV can be ascribed to the absorbed water on the surface of the fluorides which is consistent with FTIR analysis. The position of F1s (684.3 eV), K2p (292.2 eV), and Co $2p_{3/2}$ (~ 775 eV) agree with those reported for CoF_2 and KF [22–24]. The analysis of the areas of these peaks gave an atomic ratio K: Co: F_3 of 1.15:1:02:2.7, in good agreement with the expected atomic ratio. Figure 5a shows the F1s binding energy occurring at 684.5, 683.3, 684.4, and 685.0 eV for $KZnF_3$, $KMnF_3$, $KCoF_3$, and $KFeF_3$, respectively. The $K2p_{3/2}$ binding energy occurred at 292.8, 293.0, 292.8, and 293.3 eV for the $KZnF_3$, $KMnF_3$, $KCoF_3$, and $KFeF_3$, respectively (Fig. 5b) and the $K2p_{1/2}$ binding energy occurred for the same compounds at 295.6, 295.7, 295.5, and 295.9 eV. Investigation of KMF_3 crystals (M = Mn, Co, Fe, Co, Ni, Cu, Zn) showed that the peaks in the XPS spectra correspond to the multiplets arising from the 3d electrons of M^{3+} ions [25]. The stationary bands found in XPS spectra are independent of the

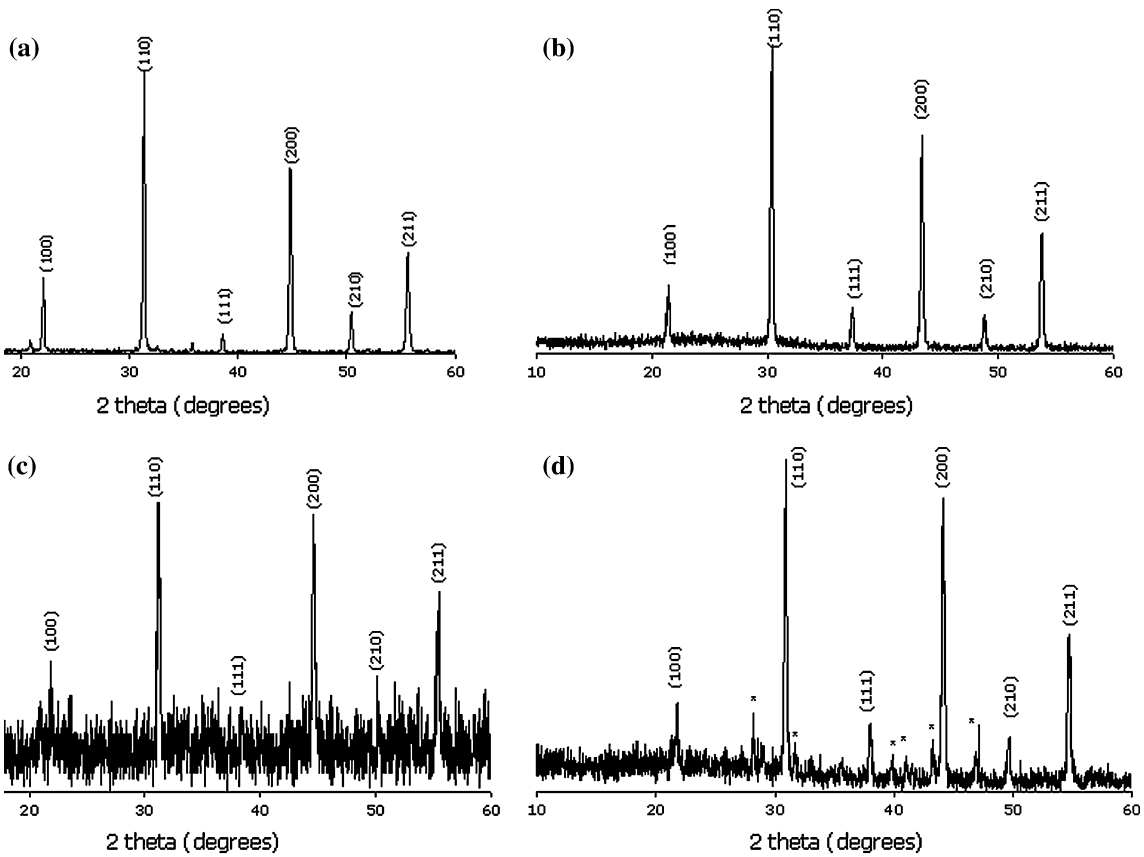

Fig. 1 Powder X-ray diffraction pattern of (**a**) $KZnF_3$, (**b**) $KMnF_3$, (**c**) $KCoF_3$, and (**d**) $KFeF_3$ synthesized by microwave hydrothermal method

Table 1 Crystal structure details of KMF_3 (M = Zn, Mn, Co, and Fe)

	a (Å)	V (Å^3)	Z	Space group
$KZnF_3$	4.055(0)	66.68	1	*Pm3m*
$KMnF_3$	4.182(0)	73.14	1	*Pm3m*
$KCoF_3$	4.070(8)	67.46	1	*Pm3m*
$KFeF_3$	4.120(0)	69.93	1	*Pm3m*

kind of M ion and are assigned to the F^- 2p valence band [26]. Though KMF_3 materials in general have ideal perovskite structure, due to the crystalline field at the surroundings of Fe^{2+} and Co^{2+} can distort the perovskite structure leading to elongation of F^- ions and reduced M–F–M inter atomic distances which can induce some covalence character. Thus the variation in the strength of M–F chemical bond via the Madelung potential could account for the variation in the binding energies (F1s, $K2p_{1/2}$, and $K2p_{3/2}$) and result in the relative shift of the F peaks of $KCoF_3$ and $KFeF_3$ (Fig. 5a) [27, 28].

In semiconductor technology, vacuum-ultraviolet transparent (VUT) materials for lenses in optical lithography are needed [29]. KMF_3 materials with perovskite structures are potential candidates and received recent attention because they do not have birefringence which makes design of lenses difficult [30]. The suitability of these materials is largely dependent on the electronic properties, which are affected by the band-gap of the material (E_g). To determine the E_g, we have performed the diffuse reflectance spectra of the $KCoF_3$ samples in the UV–VIS–NIR range (Fig. 6). The diffuse reflectance data of Fig. 6a was used to calculate the absorption coefficient from the Kubelka-Munk (KM) function [31, 32] defined as:

$$F(R_\infty) = \frac{\alpha}{S} = \frac{(1-R_\infty)^2}{2R} \quad \text{where} \quad R_\infty = \frac{R_{\text{sample}}}{R_{\text{PTFE}}}.$$

Here "α" is the absorption coefficient, "S" the scattering coefficient, and $F(R_\infty)$ is the KM function. The energy dependence of the material in the UV–VIS–NIR was further explored. The energy dependence of semiconductors near the absorption edge is expressed as:

$$\alpha E = K(E - E_g)^\eta.$$

Here "E" is the incident photon energy ($h\nu$), "E_g" the optical absorption edge energy, "K" a constant, and the exponent "η" is dependent on the type of optical transition as a result of photon absorption [33]. The η is assigned a value of 1/2, 3/2, 2, and 3 for direct allowed, direct

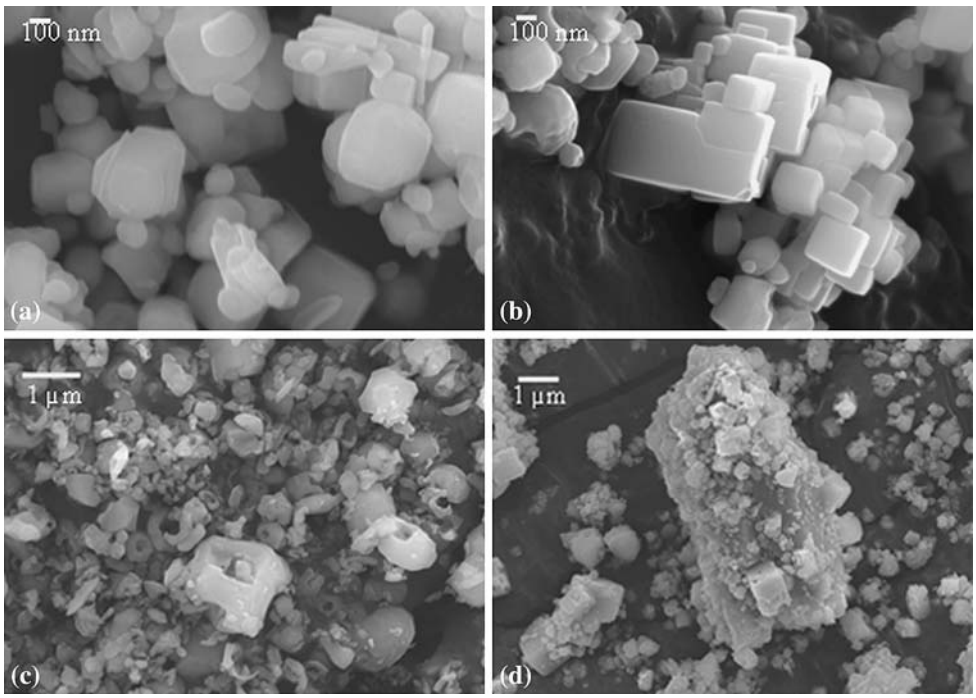

Fig. 2 SEM images of (**a**) $KZnF_3$, (**b**) $KMnF_3$, (**c**) $KCoF_3$, and (**d**) $KFeF_3$ synthesized by microwave hydrothermal method

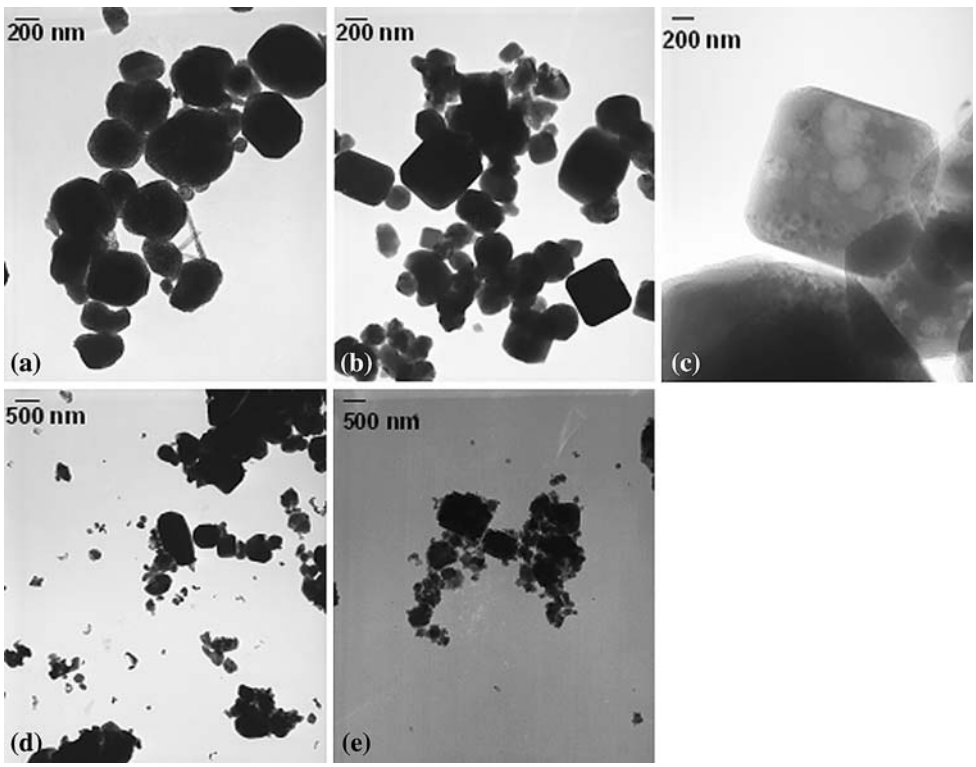

Fig. 3 TEM images for $KZnF_3$ (**a**), $KMnF_3$ (**b** and **c**), $KCoF_3$ (**d**), and $KFeF_3$ (**e**) materials showing cubic morphologies

forbidden, indirect allowed, and indirect forbidden transition, respectively [34]. For the diffused reflectance spectra, KM function can be used instead of "α" for estimation of the optical absorption edge energy [33]. It was observed that a plot of $F(R_\infty)\ E$ vs. E was linear near the edge for direct allowed transition ($\eta = 1/2$). The intercept of the line on abscissa ($F(R_\infty)\ E = 0$) gave the value of optical absorption edge energy to be 2.2 ± 0.2 eV for $KCoF_3$. Figure 6b shows the plot of the same. The E_g determined is in agreement with the E_g predicted (2.4) from modeling studies using the local spin density approximation approach [35]. The results indicate $KCoF_3$ are insulators

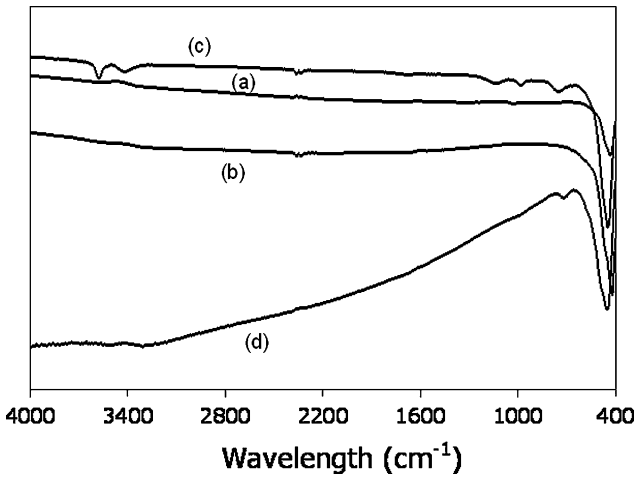

Fig. 4 F1s and K2p XPS plot of (a) $KZnF_3$, (b) $KMnF_3$, (c) $KCoF_3$, and (d) $KFeF_3$

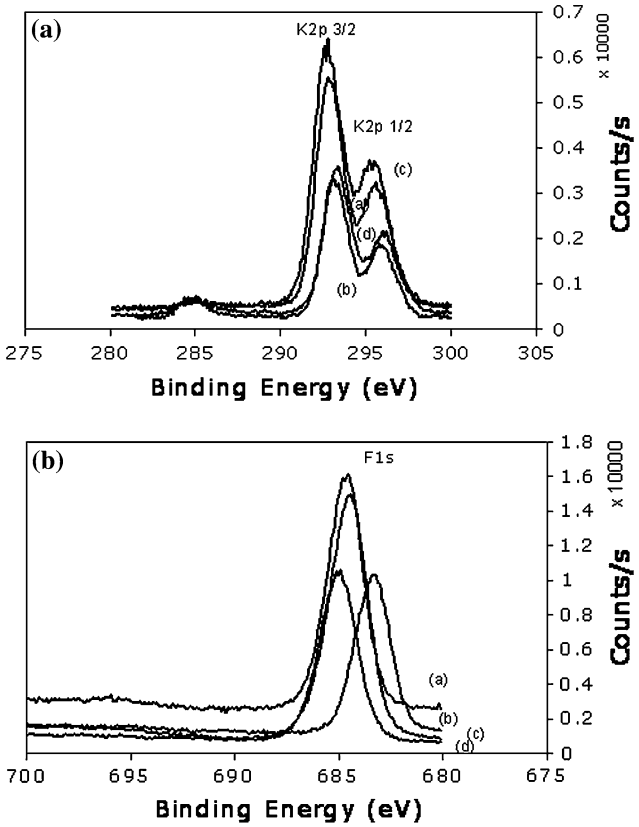

Fig. 5 FTIR spectra of (**a**) $KZnF_3$, (**b**) $KMnF_3$, (**c**) $KCoF_3$, and (**d**) $KFeF_3$

and the size of the energy gap is determined by increased charge transfer energy caused by the more ionic nature of Co–F bonding. The diffused reflectance spectra for direct band-gap orthorhombic (β) Ta_2O_5 [36] prepared by heating Ta metal in air is also recorded for comparison. The value of optical absorption edge energy for indirect allowed

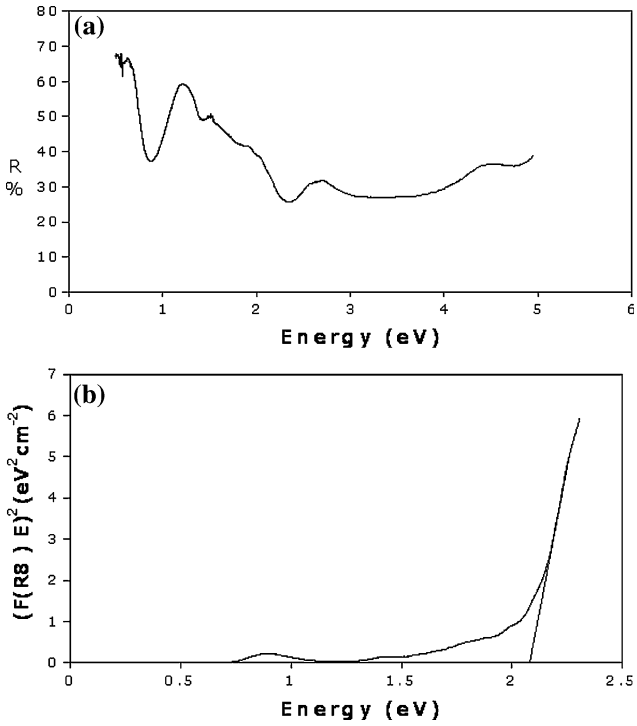

Fig. 6 (**a**) Diffuse reflectance spectra of $KCoF_3$ in the wavelength range 250–2500 nm. (**b**) Plot of $F(R_\infty)$ vs. E (eV) for the estimation of the optical absorption edge energy

transition for Ta_2O_5 was found to be 4.0 ± 0.2 eV, which is consistent with those seen for the β-Ta_2O_5 reported [37].

Conclusions

Microwave hydrothermal synthesis has been successfully applied for the synthesis of nano-sized complex metal fluorides of KMF_3 type (M = Zn, Mn, Co, Fe). The proposed method is simple, less labor intensive, and less time consuming. The products were characterized for structural, chemical, and optical properties. The optical transition band-gap of the $KCoF_3$ was determined to be 2.2 eV. Efforts to optimize the synthesis conditions (time, power output of the microwave) to eliminate the impurities associated with $KFeF_3$ materials are in progress and the results will be communicated in future.

Acknowledgements The authors would like to acknowledge Professor Allan Kirkpatrick, Department Head, Mechanical Engineering, Colorado State University, for his continued help, encouragement, and support.

References

1. Scott JF (1988) Ferroelectr Rev 1:1
2. Millis JF (1988) Nature 392:147. doi:10.1038/32348
3. Wessles BW (1995) Annu Rev Mater Sci 25:525

4. Dzik GD, Sokolska I, Golab S, Baluka M (2000) J Alloy Comp 300:254. doi:10.1016/S0925-8388(99)00779-3
5. Su H, Jia Z, Shi C (2002) Chem Mater 14:310. doi:10.1021/cm010648q
6. Somiya S, Hirano SI, Yoshimura M, Yanagisawa K (1981) J Mater Sci 16:813. doi:10.1007/BF02402800
7. Zhao C, Feng S, Xu R, Shi C, Ni J (1997) Chem Commun (Camb) 10:945. doi:10.1039/a607066c
8. Zhao C, Feng S, Chao Z, Shi C, Xu R, Ni J (1996) Chem Commun (Camb) 14:1641. doi:10.1039/cc9960001641
9. Hua R, Jia Z, Xie D, Shi C (2002) Chem Lett 31:538. doi:10.1246/cl.2002.538
10. Lee J, Shin H, Lee J, Chung H, Zhang Q, Saito F (2003) Mater Trans 44:1457. doi:10.2320/matertrans.44.1457
11. Sreeja V, Joy PA (2007) Mater Res Bull 42:1570. doi:10.1016/j.materresbull.2006.11.014
12. Kumada N, Kinomura N, Komarneni S (1998) Mater Res Bull 33:1411. doi:10.1016/S0025-5408(98)00116-0
13. Komarneni S, Roy R, Li QH (1992) Mater Res Bull 27:1393. doi:10.1016/0025-5408(92)90004-J
14. Komarneni S, Li QH, Roy R (1994) J Math Chem 4:1903. doi:10.1039/jm9940401903
15. Komarneni S, Katsuki H (2002) Pure Appl Chem 74:1537. doi:10.1351/pac200274091537
16. Liu J, Li K, Wang H, Zhu M, Yan H (2004) Chem Phys Lett 396:429. doi:10.1016/j.cplett.2004.08.094
17. Khollam YB, Deshpande AS, Patil AJ, Potdar HS, Deshpande SB, Date SK (2001) Mater Chem Phys 71:235. doi:10.1016/S0254-0584(01)00287-5
18. Baldassari S, Komarneni S, Mariani E, Villa C (2005) Mater Res Bull 40:2014. doi:10.1016/j.materresbull.2005.05.023
19. Verma S, Joy PA, Khollam YB, Potdar HS, Deshpande SB (2004) Mater Lett 58:1092. doi:10.1016/j.matlet.2003.08.025
20. Kim C-K, Lee J-H, Katoh S, Murakami R, Yoshimura M (2001) Mater Res Bull 36:2241. doi:10.1016/S0025-5408(01)00703-6
21. Card No JCPDS 72–113, 72–109, 18–1006, 72,110, ICDD, PCPDFWIN v.2.1, JCPDS-International centre for diffraction data 2000
22. Chastain J (1992) Handbook of X-ray photoelectron spectroscopy. Perkin, Eden Prairie, MN, USA
23. Fadley CS, Shirley DA, Freeman AG, Bagus PS, Mallow GV (1969) Phys Rev Lett 24:1397. doi:10.1103/PhysRevLett.23.1397
24. Kowalcyyk SP, Ley L, McFeely FR, Shirley DA (1977) Phys Rev B 15:4997. doi:10.1103/PhysRevB.15.4997
25. Sugawara F, Onuki H (1978) J Phys Soc Jpn 44:1045. doi:10.1143/JPSJ.44.1045
26. Onuki H, Sugawara F, Hirano M, Yamaguchi Y (1976) J Phys Soc Jpn 41:1807. doi:10.1143/JPSJ.41.1807
27. Okazaki A, Suemune Y (1962) J Phys Soc Jpn 17:204
28. Sugano S, Shulman RG (1963) Phys Rev 130:517. doi:10.1103/PhysRev.130.517
29. Sahnoun M, Zbiri M, Daul C, Khenata R, Baltache H, Driz M (2005) Mater Chem Phys 91:185. doi:10.1016/j.matchemphys.2004.11.019
30. Horsch G, Paus P (1986) J Opt Commun 60:89. doi:10.1016/0030-4018(86)90119-7
31. Kubelka P, Munk F (1931) Z Tech Phys 12:593
32. Kortum G (1969) Reflectance spectroscopy principles methods, applications. Spinger-Verlag, New York
33. Barton DG, Shtein M, Wilson RD, Soled SL, Iglesia E (1999) J Phys Chem B 103:630. doi:10.1021/jp983555d
34. Tauc J, Grigorov R, Vancu A (1966) Phys Status Solidi 15:627. doi:10.1002/pssb.19660150224
35. Punkkinen MPJ (1999) Solid State Commun 11:477. doi:10.1016/S0038-1098(99)00239-2
36. Sahu BR, Kleinman L (2004) Phys Rev B 69:165202. doi:10.1103/PhysRevB.69.165202
37. Knausenberger WH, Tauber RN (1973) J Electrochem Soc 129:927. doi:10.1149/1.2403602